

Received August 13, 2020, accepted August 16, 2020, date of publication August 18, 2020, date of current version August 28, 2020.

Digital Object Identifier 10.1109/ACCESS.2020.3017679

Modal Analysis and Structure Optimization of Permanent Magnet Synchronous Motor

JIAN ZHAO¹, ZHIBIN WANG¹, HAIQIANG LIU¹, FAN NING¹, XUEWU HONG¹, JINGJUAN DU¹, AND MING YU^{1,2}

¹School of Control and Mechanical Engineering, Tianjin Chengjian University, Tianjin 300384, China

²School of Computer and Information Engineering, Tianjin Chengjian University, Tianjin 300384, China

Corresponding author: Ming Yu (maxyuming@163.com)

This work was supported in part by the Natural Science Foundation of Tianjin under Grant 16JCZDJC38600, in part by the Natural Science Foundation of China under Grant 51707128, and in part by the Tianjin Technology Commissioner Project under Grant 19JCTPJC49000.

ABSTRACT Permanent magnet synchronous motors are the core components of electric vehicles and widely used in the field of electric vehicles. The existence of vibration will reduce the operating efficiency and service life of the motor, which is the key factor to determine whether the motor is running normally. In this article, a certain type of permanent magnet synchronous motor is taken as the test object. The permanent magnet synchronous motor is divided into three substructures: stator, rotor and shell. The finite element modal results are obtained respectively. The modal parameters of the whole PMSM are calculated by using the substructure modal synthesis method. The weak links of the motor are found out and the structure optimization is carried out. Through the calculation of the modal analysis, it can be seen that each vibration mode of the optimized motor has been reduced, and the amplitude difference between the 2nd order and the 5th order is the largest. Finally, the modal test is carried out on the motor using the exciter method, the test results are analyzed, and the modal parameters of the motor are obtained through the frequency domain analysis method, the FEA result is confirmed by the modal test of the motor.


INDEX TERMS Experimental modal analysis, modal synthesis method, permanent magnet synchronous motor, structure optimization.

I. INTRODUCTION

Permanent magnet synchronous motors have a broad application prospects in the field of electric vehicles due to their high efficiency, high power density, high power factor, and high controllability. As a driving tool with special structure and function, the permanent magnet synchronous motor is used in complex environments to meet specific needs. The permanent magnet synchronous motor gradually develops towards the lightweight design of high power density, and its structure gradually moves closer to diversification and miniaturization, and gradually replaces the traditional motors in electric vehicles. However, they also face problems such as complex structure, reduced rigidity, and difficulty in suppressing electromagnetic vibration. Due to the complicated structure of permanent magnet synchronous motors, it is easy to damage the permanent magnet materials due to vibration [1]. In severe cases, noise pollution will be occur, the driving comfort of

the car and the performance of permanent magnets will be reduced. It is very important to study the vibration characteristics of motor.

Over the past decades, a considerable amount of intensive research has focused on the structural characteristics of motors. Moayyedi [2] proposed an improved reduced order modeling method, which is based on the proper orthogonal decomposition (POD) method. The results obtained from the calibrated reduced-order model show that the model established by this method has high accuracy. Meng [3] used Pro/E modeling: through appropriate assumptions and equivalent treatments on the stator, rotor core and coil windings of the motor, the finite element simulation model of each component was established, and the workbench was used to analyze the calculation of each stage of the motor Modal, to obtain the modal frequency of each modal. The modal test of the motor was carried out by the hammering method, and the comparative analysis results were used to guide the design of the motor. However, if the hammer excitation energy is too small, high frequency modals will

The associate editor coordinating the review of this manuscript and approving it for publication was Hamid Mohammad-Sedighi .

be missed. Gaur [4] proposed a new approach for nonlinear finite element analysis. The methodology was very suitable and gives very accurate results in linear as well as in nonlinear range of the material behavior. The methodology eliminates the lengthy and tedious procedure of step by step and then iterative procedure adopted classically for nonlinear analysis problems. The experiments results shows that this method is only suitable for nonlinear analysis of materials. Yin [5] has done a lot of research on the modal analysis of stator core and winding, and proposed a new stator system analysis model, which can effectively analyze the 0th-order mode and improve the model calculation efficiency. The modal tests of the stator core and stator core-winding system were carried out by hammering method, and the validity of the finite element analysis model was verified. Rahman [6] established a mathematical model of a forced nonlinear vibration of Euler-Bernoulli beam resting on nonlinear elastic foundation. the nonlinear vibration behavior of the beam was studied by using an improved multi-level residual harmonic balance method, at the same time, the influence of excitation parameters on nonlinear vibration behavior was also studied. Feng [7] and others adopted the modal synthesis method to solve the body modal, the response of the body structure under engine excitation and the acoustic response of the body structure coupled with the cab acoustic cavity. The results show that the modal synthesis method can greatly reduce the calculation time. Sibasish [8] designed and analyzed the concentrated winding synchronous reluctance motor, and determined the structure size of the fixed rotor and calculated the winding parameters. Hieu [9] proposed to use the equivalent linearization method with a weighted averaging to analyze the transverse vibration of quintic nonlinear Euler-Bernoulli beams subjected to axial loads. And the impact of nonlinear terms on the dynamical behavior of beams and the effect of the initial amplitude on frequencies of beams were investigated. Yan [10] proposed an improved method of free interface modal synthesis. After substructure modal synthesis of the structure, the modal parameters of the reduced-order model were obtained, and then the sensitivity of the model eigenvalues to the design variables was used. The gradient was constructed to modify the wing structure model, which greatly improves the calculation efficiency. Xie [11] took the three-phase induction motor as the research object, proposed an optimal design scheme of the stator winding based on the characteristics of the stator winding connection of the motor. The electromagnetic vibration and vibration reduction of the improved motor were studied, and the optimized scheme was verified in Reduce the feasibility of electromagnetic vibration. Marashi [12] proposed a Short Time Transmissibility Measurement that does not rely on excitation characteristics. the modal shape of the bridge can be accurately measured and calculated, and the robustness of the method is investigated. Wang [13] studied the electromagnetic noise characteristics of a permanent magnet synchronous motor for electric vehicle driving based on theoretical analysis and Ansys multiphysics finite element analysis platform,,

the electromagnetic noise characteristics of the motor was optimized and obtained through Acoustics finite element simulation analysis. Qiao [14] proposed an electromagnetic design and analysis method of the six-phase fractional slot concentrated winding permanent magnet motor, a 20kW 48slots 44 poles six-phase fractional-slot concentrated winding permanent magnet motor prototype was designed and manufactured, and its electromagnetic performance and vibration performance was tested, the test results are in good agreement with the calculated results. Kong [15] obtained the electromagnetic vibration of motors under different loads by analyzing the amplitude of the electromagnetic force wave. According to the modal analysis of the stator core, in the absence of resonance, the vibration response value will increase when the electromagnetic force of the harmonics in the first and second order slots increases.

In this article, a certain type of permanent magnet synchronous motor is taken as the research object. The free-interface modal synthesis method is used to analyze the modal of the permanent magnet synchronous motor, and the calculated modal parameters of the motor are obtained. The low-order natural frequency and vibration shape of the permanent magnet synchronous motor are obtained by building a modal test system and using the vibration exciter method to perform a modal test on the permanent magnet synchronous motor, and the finite element results are verified; Finally, the scheme of removing the stiffeners to optimize the structure of the permanent magnet synchronous motor is proposed and verified by experiments.

TABLE 1. Main parameters of Permanent magnet synchronous motor.

Parameter	Numerical value
Number of poles	6
Number of slots	36
Rated voltage/V	110
Rated power/kW	30
Rated speed/r·min ⁻¹	4500
Outer diameter of stator/mm	170
Outer diameter of rotor/mm	127
Magnetic steel thickness/mm	5

II. MODAL SYNTHESIS ANALYSIS OF PERMANENT MAGNET SYNCHRONOUS MOTOR

A. MODAL ANALYSIS OF PERMANENT MAGNET SYNCHRONOUS MOTOR SUBSTRUCTURE

A 6-pole 36-slot permanent magnet synchronous motor is taken as the research object selected in this article. The basic parameters are shown in Table 1. The structure of a 6-pole 36-slot rotor is shown in Fig 1.

First of all, the permanent magnet synchronous motor is divided into three independent sub-structures of stator, rotor and shell according to the structural characteristics. The models are established separately by using 3D software, and the simplified consideration of the equivalent model is

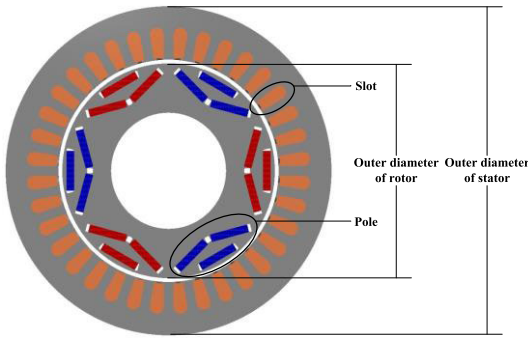


FIGURE 1. Structure drawing of 6-pole 36 slot rotor.

considered, the parts of the cooling system joints and rounded corners that have little influence on the model calculation are ignored. The substructure of the permanent magnet synchronous motor is shown in Fig 2.

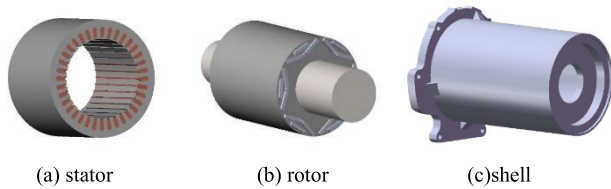


FIGURE 2. Substructure of motor. (a) Stator model, (b) Rotor model, and (c) Shell model.

TABLE 2. Material properties of motor substructure.

Substructure	Modulus of elasticity	Material density	Poisson's ratio
stator	2.1E11	7800kg/m ³	0.3
rotor	2.1E11	7800kg/m ³	0.3
Shell	7E10	3000kg/m ³	0.3

The generated substructure model is imported into the finite element software, and their material properties are set respectively. The material properties of the substructure are shown in Table 2, and the mesh is divided, and the stress concentration area is refined. The finite element model is generated as shown in Fig 3.

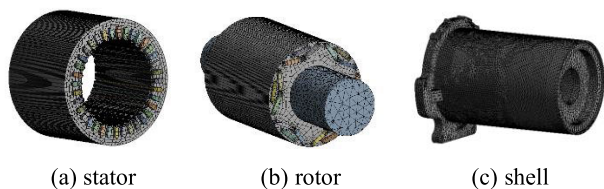


FIGURE 3. Substructure finite element model. (a) Stator finite element model, (b) Rotor finite element model, and (c) Shell finite element model.

The permanent magnet synchronous motor can be regarded as a multi-degree-of-freedom vibration system.

Generally, the motion differential equation for a multi-degree-of-freedom system is:

$$M\ddot{x} + C\dot{x} + Kx = F(t) \tag{1}$$

where, M denotes the mass matrix; C denotes the damping matrix; K denotes the stiffness matrix; $F(t)$ denotes the excitation force; x denotes the displacement vector.

Because the motor is a metal structure, the damping is small, and the effect on the natural frequency and mode shape is very small, so it can be ignored, and the undamped vibration system equation is as follows:

$$M\ddot{x} + Kx = 0 \tag{2}$$

The corresponding characteristic equation is:

$$(K - \omega^2 M)x = 0 \tag{3}$$

According to the theory of linear equations, the necessary and sufficient conditions for non-zero solutions is $|K - \omega^2 M| = 0$, a series of discrete roots like ω_i^2 ($i = 1, 2, 3, \dots, n$) and non-zero solution vectors like x_i ($i = 1, 2, 3, \dots, n$) can be solved. Among them, ω_i^2 and x_i are the natural frequency and vibration mode of the permanent magnet synchronous motor.

The Block Lanczos method is used to extract the modes. The superelement data of the stator, rotor, and shell are solved separately, and the modal frequencies and modes of the superelement are saved. The modal frequencies of the substructures are shown in Table 3, and the modal shapes are shown in Fig 4.

TABLE 3. Modal frequencies of substructures.

Order	Stator [Hz]	rotor [Hz]	shell [Hz]
1	5107.6	1262.6	2039.7
2	5558.5	2761.1	3285.7
3	5563.3	4111.1	3352.5
4	6704.6	5651.1	3785.7
5	9596.3	6939.7	4004.8
6	9977.5	9353.9	4276.2

B. MODAL SYNTHESIS RESULT OF PERMANENT MAGNET SYNCHRONOUS MOTOR

The basic idea of the substructure modal synthesis method [7], [10] is to divide a large complex system into several substructures according to its structural characteristics, and perform model reduction processing on the substructure modal matrix in a certain way, and then reduce the substructure after the reduction process. The structural modal matrix is recombined to solve the overall system [16].

The free-interface mode synthesis method uses the low-order mode set and the residual mode set to construct the hypothetical mode set of the substructure. Take the interface force as the generalized coordinates of the substructure, and eliminate this group of generalized coordinates through the displacement coordination condition. The comprehensive

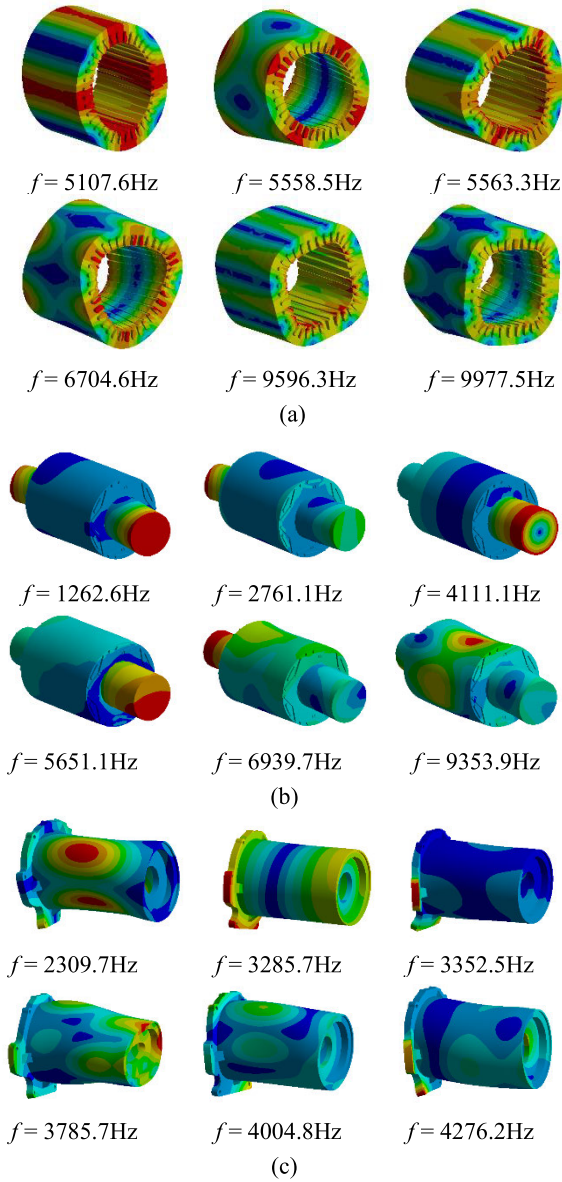


FIGURE 4. Modal shape of substructure. (a) Stator mode shape, (b) Rotor mode shape, and (c) Shell mode shape.

calculation efficiency of the system with a large number of interface degrees of freedom has been effectively improved. Compared with the fixed interface mode synthesis method, the free interface mode synthesis method is more convenient to be combined with the physical test, the free interface mode synthesis method is used to analyze the dynamic performance of the permanent magnet synchronous motor in this article [17]. The basic principle is as follows:

The simply supported beam structure is used as an example to illustrate, as shown in Fig 5, the beam structure is divided into two substructures α, β . Its physical coordinate set $\{u\}$ is divided into internal coordinate set $\{u_i\}$ and contact surface coordinate set $\{u_j\}$,

$$\{u^\alpha\} = \begin{Bmatrix} u_i^\alpha \\ u_j^\alpha \end{Bmatrix} \quad \{u^\beta\} = \begin{Bmatrix} u_i^\beta \\ u_j^\beta \end{Bmatrix} \quad (4)$$

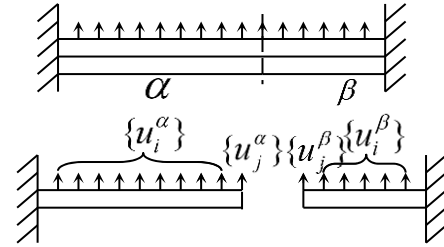


FIGURE 5. Simple supported beam model of free interface.

where

$\{u^\alpha\}$ is the physical coordinate set of the substructure α ;
 $\{u^\beta\}$ is the physical coordinate set of the substructure β ;
 u_i^α is the internal coordinate set of the substructure α ;
 u_i^β is the internal coordinate set of the substructure β ;
 u_j^α is the coordinate set of the contact surface of the substructure α ;
 u_j^β is the coordinate set of the contact surface of the substructure β .

Contact displacement condition [18]: $\{u_j^\alpha\} = \{u_j^\beta\}$

The modal matrix of each substructure is assumed to be $[\varnothing^\alpha]$ and $[\varnothing^\beta]$ respectively, modal coordinates $\{p\} = \begin{Bmatrix} p^\alpha \\ p^\beta \end{Bmatrix}$, So there are:

$$\begin{Bmatrix} u_i^\alpha \\ u_j^\alpha \end{Bmatrix} = \begin{bmatrix} \varnothing_i^\alpha \\ \varnothing_j^\alpha \end{bmatrix} \{p^\alpha\} \quad \begin{Bmatrix} u_i^\beta \\ u_j^\beta \end{Bmatrix} = \begin{bmatrix} \varnothing_i^\beta \\ \varnothing_j^\beta \end{bmatrix} \{p^\beta\} \quad (5)$$

where

\varnothing_i^α is the modal matrix inside the substructure α ;
 \varnothing_i^β is the modal matrix inside the substructure β ;
 \varnothing_j^α is the modal matrix of the α contact surface of the substructure;
 \varnothing_j^β is the modal matrix of the β contact surface of the substructure;
 p^α is the modal coordinate of the substructure α ;
 p^β is the modal coordinate of the substructure β ;

Record:
$$[\overline{M}] = \begin{bmatrix} [\overline{M}^\alpha] & 0 \\ 0 & [\overline{M}^\beta] \end{bmatrix}, [\overline{K}] = \begin{bmatrix} [\overline{K}^\alpha] & 0 \\ 0 & [\overline{K}^\beta] \end{bmatrix},$$

at the same time:

$$\begin{aligned} [\overline{M}^\alpha] &= [\varphi^\alpha]^T [m^\alpha] [\varphi^\alpha] \\ [\overline{M}^\beta] &= [\varphi^\beta]^T [m^\beta] [\varphi^\beta] \\ [\overline{K}^\alpha] &= [\varphi^\alpha]^T [k^\alpha] [\varphi^\alpha] \\ [\overline{K}^\beta] &= [\varphi^\beta]^T [k^\beta] [\varphi^\beta] \end{aligned} \quad (6)$$

$$\begin{aligned} [\overline{M}^\alpha] &= [\varphi^\alpha]^T [m^\alpha] [\varphi^\alpha] \\ [\overline{M}^\beta] &= [\varphi^\beta]^T [m^\beta] [\varphi^\beta] \\ [\overline{K}^\alpha] &= [\varphi^\alpha]^T [k^\alpha] [\varphi^\alpha] \\ [\overline{K}^\beta] &= [\varphi^\beta]^T [k^\beta] [\varphi^\beta] \end{aligned} \quad (7)$$

where

$[\overline{M}^\alpha]$ is the mass matrix after substructure α is reduced;
 $[\overline{M}^\beta]$ is the reduced mass matrix of the substructure β ;
 $[\overline{K}^\alpha]$ is the stiffness matrix after substructure α is reduced;
 $[\overline{K}^\beta]$ is the stiffness matrix of the reduced substructure β ;

$[\varphi^\alpha]$ is the coordinate transformation matrix of substructure α ;

$[\varphi^\beta]$ is the coordinate transformation matrix of substructure β ;

$[m^\alpha]$ is the mass matrix of substructure α ;

$[m^\beta]$ is the mass matrix of substructure β ;

$[k^\alpha]$ is the stiffness matrix of substructure α ;

$[k^\beta]$ is the stiffness matrix of substructure β ;

The displacement conditions of (4) and contact surface are as follows:

$$[\varphi_j^\alpha] \{p^\alpha\} = [\varphi_j^\beta] \{p^\beta\} \quad (8)$$

The form of constraint equation is as follows:

$$[C] \{p\} = 0 \quad [C] = \begin{bmatrix} [\varphi_j^\alpha] & -[\varphi_j^\beta] \end{bmatrix} \quad (9)$$

where

$[C]$ is the difference between the substructure α and β contact surface modal matrix;

Carry out the second coordinate transformation, and block $\{p\}$ into:

$$\{p\} = \begin{Bmatrix} p_d \\ p_I \end{Bmatrix} \quad [[C_{dd}][C_{dI}]] \begin{Bmatrix} p_d \\ p_I \end{Bmatrix} = \{0\} \quad (10)$$

$$\{p_d\} = -[C_{dd}]^{-1} [C_{dI}] \{p_I\} \quad (11)$$

$$\{p\} = \begin{bmatrix} -[C_{dd}]^{-1} [C_{dI}] \\ I & 0 \end{bmatrix} \{p_I\} = [S] \{q\} \quad (12)$$

$$[S] = \begin{bmatrix} -[C_{dd}]^{-1} [C_{dI}] \\ I & 0 \end{bmatrix} \quad (13)$$

where

$[S]$ is the independent coordinate transformation matrix;

$$[M] = [S]^T [\overline{M}] [S] \quad [K] = [S]^T [\overline{K}] [S] \quad (14)$$

where

$[M]$ is the overall structural modal comprehensive mass matrix;

$[K]$ is the overall structural modal comprehensive stiffness matrix;

According to the Lagrangian equation, the free vibration equation of the integrated mode of the beam structure is as follows:

$$[M] \{\ddot{q}\} + [K] \{q\} = \{0\} \quad (15)$$

where

$\{q\}$ is the displacement vector;

$\{\ddot{q}\}$ is the acceleration vector;

Then the generalized eigenvalue problem is obtained as follows:

$$([K] - \omega^2 [M]) \{\psi\} = \{0\} \quad (16)$$

where

$\{\psi\}$ is the main mode matrix;

From formula (16), the characteristic equation is $|[K] - \omega^2 [M]| = 0$, The characteristic equation is an n th-order polynomial about ω^2 , A set of discrete solutions can be obtained such as $\omega_1^2, \omega_2^2, \dots, \omega_n^2$, the n undamped natural frequencies of the system can be composed of the square roots of these n solutions. Put the obtained undamped natural frequency ω_i^2 into the equation (13), the value of $\{\psi\}$ can be solved, and the i -th mode vector can be obtained at the same time.

The dynamic performance of the whole structure can be obtained by solving it [19].

Through the modal analysis of the stator, rotor, and shell, the sub-structure modal is extracted to generate the super-element model. The free interface modal synthesis method is used. When the sub-structure super-element data is called, the modal of the permanent magnet synchronous motor machine the order is less than the modal order obtained by each substructure. Since the three substructures are all solids, TARGE170 and CONTA173 contact pairs are used in ANSYS to generate a three-dimensional model of the whole machine and solve the whole machine model. The simply supported beam structure is used as an example to illustrate, as shown Fig 6. The modal frequency of the permanent magnet synchronous motor is listed in Table 4, and the modal shape is shown in Fig 6.

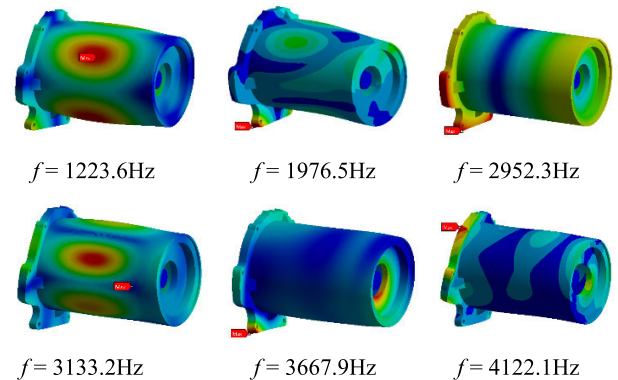


FIGURE 6. Motor mode shapes.

TABLE 4. Modal synthesis frequency of motor.

Order	Frequency (f/Hz)	Relative deformation (x/mm)
1	1223.6	0.264
2	1976.5	0.362
3	2952.3	0.302
4	3133.2	0.323
5	3667.9	0.405
6	4122.1	0.372

For permanent magnet synchronous motors, the low-order natural frequencies and mode shapes are the most important factors, and the modal quality occupied by the low-order modes in the modal analysis is large, which has a great

impact on the vibration of the structure. The dynamic characteristics of the structure play a decisive role, so the modal analysis of the motor only requires the first few natural frequencies and vibration modes to meet the requirements of the modal analysis of the motor.

The 6-order modal frequency and mode shape of the permanent magnet synchronous motor are obtained from the sub-structure mode synthesis. We observed that a first-order squeeze bending deformation appears in the middle of the shell at 1223.6 Hz; the end cover position First-order squeeze bending deformation occurs at 1976.5Hz; the deformation mainly occurs at both ends of the motor, and we observed that the torsional deformation at 2952.3 Hz; first-order bending deformation occurs in the middle of the housing at 3133.2 Hz; the deformation is mainly generated at the end, which is a first-order bending deformation at 3667.9 Hz; we observed that a second-order bending deformation at the end of the shell at 4122.1 Hz. The deformation amplitude at 3667.9 Hz is the largest and the deformation is the most severe.

The efficiency of the motor is equal to the ratio of output power to input power. The main factors affecting motor efficiency are copper loss, iron loss and mechanical loss. Mechanical loss mainly includes friction loss, air loss and vibration loss. Large deformation of the motor output shaft end cover will increase the vibration loss, that is, the efficiency of the motor will decrease, so it is necessary to optimize the structure of the motor.

III. STRUCTURE OPTIMIZATION OF PERMANENT MAGNET SYNCHRONOUS MOTOR

Through the modal analysis of the permanent magnet synchronous motor and observing the vibration pattern cloud, it can be seen that the low-order modal deformation of the permanent magnet synchronous motor mostly occurs near the output shaft end cover, including bending deformation and torsional deformation, and the deformation in this area is more obvious than other areas. Therefore, it is judged that this area is a weak area of the permanent magnet synchronous motor.

Based on the above analysis, the structure of the permanent magnet synchronous motor is optimized in this article, which focuses on the optimization of the output shaft end cover of the permanent magnet synchronous motor. Reinforcing rib is a local structure that can strengthen the strength and rigidity of the component itself without increasing the wall thickness of the component. The reinforcement in the permanent magnet synchronous motor is designed to enhance the strength of the output shaft end cover, while reduces the motor Modal frequency, and the amplitude of each mode of the motor in the area near the output shaft end cover increases. Therefore, a method to optimize the output shaft end cover of the permanent magnet synchronous motor by removing the stiffener is proposed. In order to ensure that the installation and use of permanent magnet synchronous motor will not be affected, the reinforcing rib on the end cover of output shaft

is deleted. The optimized permanent magnet synchronous motor is shown in Fig 7.

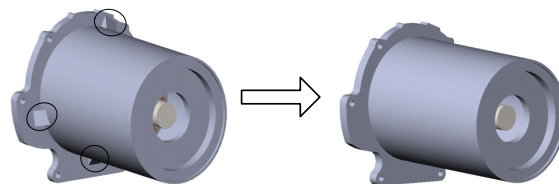


FIGURE 7. Structure optimization of permanent magnet synchronous motor.

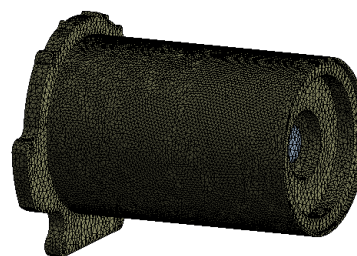


FIGURE 8. Optimized motor meshing.

The optimized permanent magnet synchronous motor is set to the same material properties as the prototype, and the computational modal analysis is performed. After optimization, the meshing of the permanent magnet synchronous motor is shown in Fig 8.

The modal frequency of the optimization permanent magnet synchronous motor is shown in Table 5, the modal vibration mode is shown in Fig 9, the comparison of the calculated modal frequency before and after the optimization of the permanent magnet synchronous motor is shown in Fig 10, and the comparison of the vibration mode amplitude is shown in the Fig 11.

TABLE 5. Modal frequency of motor after optimization.

Order	Frequency (/Hz)	Relative deformation (x/mm)
1	1525.4	0.232
2	2156.7	0.226
3	3153.6	0.265
4	3298.3	0.272
5	3823.4	0.258
6	4356.3	0.321

Comparing the natural frequency of the permanent magnet synchronous motor before and after optimization, we observed that the frequency of each step of the motor after optimization is improved, and the increase of the low-order mode is most obvious; According to the mode shapes of each order, it shows that the relative deformation in each order of the optimized permanent magnet synchronous motor has been reduced. And the deformation near the output shaft end

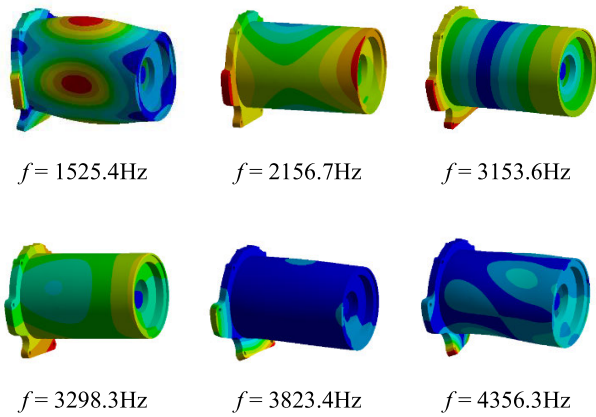


FIGURE 9. Motor mode shapes.

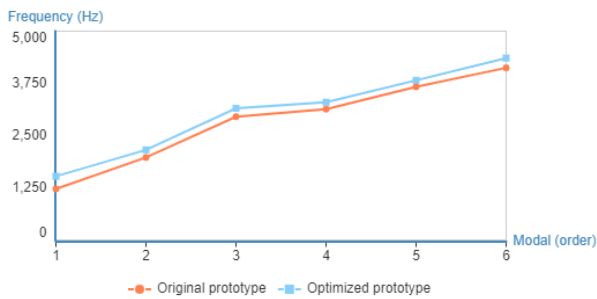


FIGURE 10. Comparison of modal frequency before and after optimization of motors.

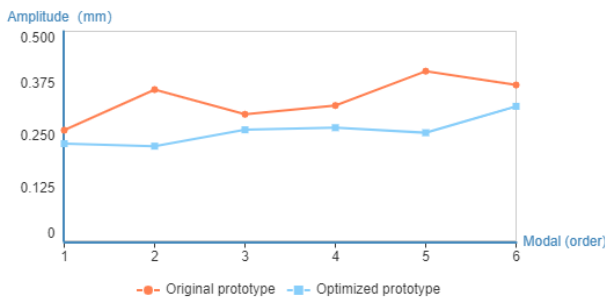


FIGURE 11. Comparison of amplitude before and after optimization of motors.

cover has been alleviated, and the modal vibration mode at the natural frequencies of the second and fifth orders has the most obvious reduction. It shows that the resonance phenomenon of the optimized permanent magnet synchronous motor is effectively avoided, but also the deformation amplitude is effectively reduced.

IV. EXPERIMENTAL MODAL ANALYSIS OF PERMANENT MAGNET SYNCHRONOUS MOTOR

In order to verify the correctness of the finite element results and the optimization method, the experimental modal analysis method is used to perform modal testing on the permanent magnet synchronous motor with the stiffener removed. Because the excitation energy of the exciter is much larger than that of the hammer and the energy distribution is more

uniform, the quality of the data is higher. At the same time, the material properties and structural characteristics of the permanent magnet synchronous motor are taken into account, the “exciter method” is used for modal testing.

The exciter method refers to an excitation method that uses a complete exciter system to conduct a modal test on the test object. The corresponding method is the hammer method. The excitation energy of the vibration exciter is much greater than that of the hammer, and the excitation force is controllable. It is the first choice for studying complex structures and nonlinear structures. The complete vibration exciter system includes signal source, power amplifier, vibration exciter, ejector rod and force sensor. Vibration exciters are classified into mechanical, electro-hydraulic, electromagnetic and piezoelectric types according to their working principles. The electromagnetic exciter is used in the test in this article.

Compared with the hammering method, the exciter method is difficult to move and inconvenient to install. Therefore, when the exciter method is used for modal testing, the exciter is usually installed for excitation, and the test is performed by moving the response sensor; The excitation position of the exciter is the modal reference point. The test in this article refers to the fixed exciter, which is tested by moving the response sensor, and the position of the modal reference point is the 15th measuring point.

The preferred method for studying complex structures. The high-strength sponge pad is used to support the permanent magnet synchronous motor and simulate the free suspension state of the permanent magnet synchronous motor. The force sensor and acceleration sensor are used to pick up the input signal and response signal respectively. The modal test system is shown in Fig 12, and the actual modal test chart is shown in Fig 13.

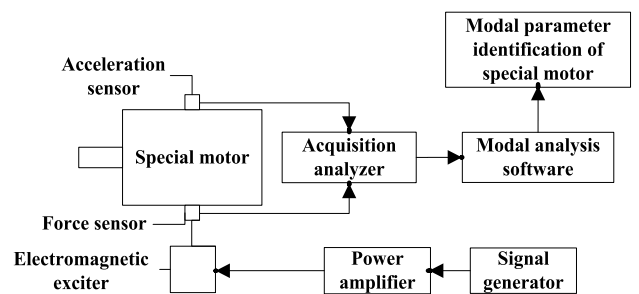


FIGURE 12. Test system diagram.

According to the principles of uniform measurement point arrangement, avoiding key nodes and loss of modals, the motor is arranged with 5 layers of measuring points in the axial direction, and 7 measuring points on each layer are evenly arranged in the axial direction to pick up the radial deformation; 1 layer of measuring points are evenly arranged on both ends of the permanent magnet synchronous motor, and each layer is also evenly arranged 7 measuring points, a total of 49 measuring points. The arrangement of measuring points is shown in Fig 14.

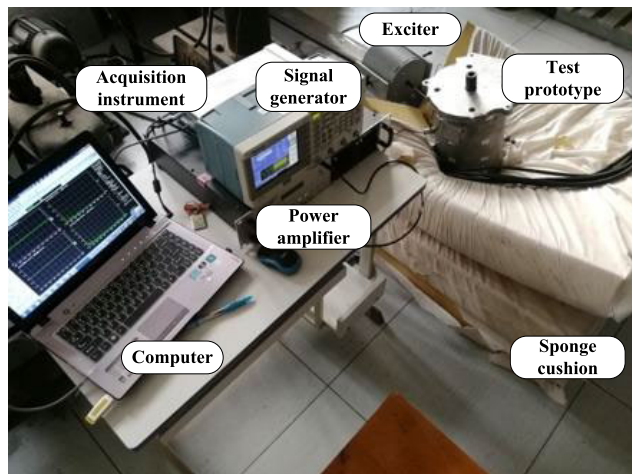


FIGURE 13. Vibration test physical diagram.

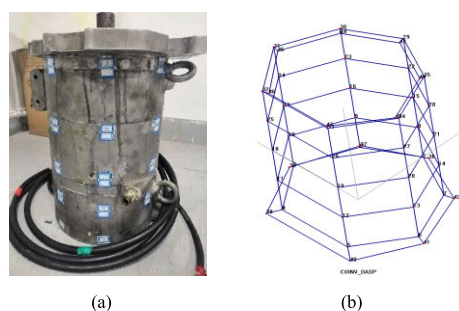


FIGURE 14. Sensor measuring point diagram. (a) Physical figure of motor measuring point, and (b) Model figure of motor measuring point.

When setting parameters, the calibration value of each channel was modified according to the calibration value of the sensor corresponding to each measurement point, and set the force sensor and acceleration sensor to the ICP coupling mode. In this test, a sinusoidal periodic signal is used, and the mode is not missed. The excitation time of a single frequency needs to be greater than 3 seconds to ensure that each frequency can be effectively excited, and each frequency section does not exceed 100 Hz, so the sampling time is set to 300 second.

TABLE 6. Test mode natural frequency.

Order	Frequency (f/Hz)	Damping ratio (%)
1	1493.4	0.159
2	2124.2	1.868
3	3098.3	1.221
4	3203.6	1.375
5	3756.5	0.994
6	4222.3	0.493

Based on the above test system, the motor modal test program is designed in this article, a single-input multi-output test method is adopted, and modal parameter identification frequency domain method [20] is used to identify motor modal parameters. The modal frequency is shown in Table 6,

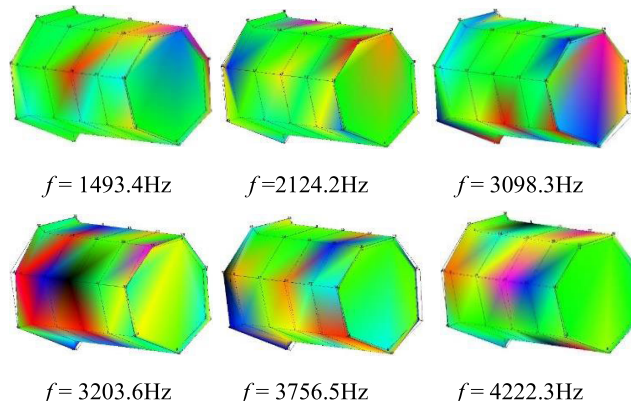


FIGURE 15. Mode shapes of the test modal of permanent magnet synchronous motor.

and the modal vibration mode is Fig 15. Comparing the vibration modes at the above frequencies, we observed that the amplitude of vibration deformation at 3756.5 Hz and 4222.3 Hz is the most obvious, and the amplitude at other frequencies is relatively small. Compare the frequencies of the two orders. We observed that the error range is only within 3.5%, the finite element results of permanent magnet synchronous motors have been verified. The comparison between the modal synthesis results of the permanent magnet synchronous motor and the modal test results is shown in Table 7.

TABLE 7. Comparison of calculated and experimental modal analysis results.

Order	Calculation of modal natural frequency [f/Hz]	Natural frequency of test mode [f/Hz]	Error [%]
1	1525.4	1473.4	3.5
2	2156.7	2124.2	1.5
3	3153.6	3098.3	1.8
4	3298.3	3203.6	2.9
5	3823.4	3756.5	1.8
6	4356.3	4222.3	3.2

V. CONCLUSION

In this article, a certain type of permanent magnet synchronous motor is taken as the research object, which is divided into three sub-structures of stator, rotor, and shell according to the structural characteristics of permanent magnet synchronous motor. The modal synthesis method is used to calculate the natural frequency and mode shape of the permanent magnet synchronous motor. The finite element analysis results are verified by the experimental modal analysis results, and an optimization scheme for permanent magnet synchronous motors is proposed. The conclusions drawn in this article are as follows:

- (1) The substructure of the permanent magnet synchronous motor is subjected to modal analysis. The free interface modal synthesis method is used to solve the modal parameters of the permanent magnet synchronous motor. The analysis shows that the weak link was

located in the end cover of the output shaft, and the relative deformation at the 2nd and 5th modal frequencies is relatively large;

- (2) The optimization method of removing the stiffeners for the output shaft end cover of the permanent magnet synchronous motor is proposed, and the modal analysis of the optimized motor is calculated. Comparing the modal parameters of the prototype and the optimized motor, we observed that the frequency of each order of the motor has been improved, and the relative deformation has been reduced.
- (3) A test modal analysis on the optimized permanent magnet synchronous motor is performed, the test results are analyzed. Compare the calculation results, the errors are all within 4%, the finite element results are verified by test results. The various steps near the output shaft end cover the amplitude of the vibration mode has been reduced, we observed that the optimization scheme adopted is correct and effective in this article.
- (4) The optimization scheme in this article only improves the exterior of the motor, only affects the motor casing and installation conditions, and has no effect on the copper loss and iron loss of the motor. The optimized motor not only increases the low-order natural frequency, but also reduces the vibration amplitude accordingly, which can reduce the vibration loss of the motor to a limited extent, so the efficiency of the optimized motor is slightly improved.

REFERENCES

- [1] T. Ishikawa, H. Inaba, and M. Matsunami, "Comparison of vibration characteristics of several interior permanent magnet synchronous motors," in *Proc. 11th ICEMS*, Wuhan, China, Oct. 2008, pp. 314–319.
- [2] M. K. Moayyedi, "Extension ability of reduced order model of unsteady incompressible flows using a combination of POD and Fourier modes," *J. Appl. Comput. Mech.*, vol. 5, no. 1, pp. 1–12, 2019, doi: [10.22055/jacm.2018.24099.1171](https://doi.org/10.22055/jacm.2018.24099.1171).
- [3] M. Bao, E. W. Chen, Y. M. Lu, Z. S. Liu, and S. Liu, "Vibration and noise analysis for a motor of pure electric vehicle," *Adv. Mater. Res.*, vols. 915–916, pp. 98–102, Apr. 2014, doi: [10.4028/www.scientific.net/AMR.915-916.98](https://doi.org/10.4028/www.scientific.net/AMR.915-916.98).
- [4] H. Gaur, "A new stress based approach for nonlinear finite element analysis," *J. Appl. Comput. Mech.*, vol. 5, no. 3, pp. 563–576, 2019, doi: [10.22055/jacm.2019.29045.1548](https://doi.org/10.22055/jacm.2019.29045.1548).
- [5] H. Yin, X. Zhang, F. Ma, C. Gu, H. Gao, and Y. Wang, "New equivalent model and modal analysis of stator core-winding system of permanent magnet motor with concentrated winding," *IEEE Access*, vol. 8, pp. 78140–78150, 2020, doi: [10.1109/ACCESS.2020.2989141](https://doi.org/10.1109/ACCESS.2020.2989141).
- [6] M. S. Rahman, "Modified multi-level residue harmonic balance method for solving nonlinear vibration problem of beam resting on nonlinear elastic foundation," *J. Appl. Comput. Mech.*, vol. 5, no. 4, pp. 627–638, 2019, doi: [10.22055/jacm.2018.26729.1352](https://doi.org/10.22055/jacm.2018.26729.1352).
- [7] H. X. Feng, "The application of mode synthesis method in the dynamic calculation of body structure," *Automot. Eng.*, vol. 34, no. 9, pp. 811–815, 2012.
- [8] S. Panda and R. K. Keshri, "Design and analysis of synchronous reluctance motor for light electric vehicle application," in *Proc. IECON 44th Annu. Conf. IEEE Ind. Electron. Soc.*, Oct. 2018, pp. 2021–2025.
- [9] D. Hieu, "Free vibration analysis of quintic nonlinear beams using equivalent linearization method with a weighted averaging," *J. Appl. Comput. Mech.*, vol. 5, no. 1, pp. 46–57, 2019, doi: [10.22055/jacm.2018.24919.1217](https://doi.org/10.22055/jacm.2018.24919.1217).
- [10] W. Yan, "Structural dynamics model updating based on substructure synthesis method," M.S. thesis, Graduate School College Aersp. Eng., Nanjing Univ. Aeronaut. Astronaut., Nanjing, China, 2014.
- [11] Y. Xie, C. Pi, and Z. Li, "Study on design and vibration reduction optimization of high starting torque induction motor," *Energies*, vol. 12, no. 7, p. 1263, Apr. 2019, doi: [10.3390/en12071263](https://doi.org/10.3390/en12071263).
- [12] S. M. Marashi, "Estimating the mode shapes of a bridge using short time transmissibility measurement from a passing vehicle," *J. Appl. Comput. Mech.*, vol. 5, no. 4, pp. 735–748, 2019, doi: [10.22055/jacm.2019.27225.1385](https://doi.org/10.22055/jacm.2019.27225.1385).
- [13] X. Y. Wang, "Research on electromagnetic vibration and noise reduction method of V type magnet rotor permanent magnet motor electric vehicles," *Proc. Chin. Soc. Electr. Eng.*, vol. 39, no. 16, pp. 4919–4926, Aug. 2019, doi: [10.13334/j.0258-8013](https://doi.org/10.13334/j.0258-8013).
- [14] M. Qiao, C. Jiang, Y. Zhu, and G. Li, "Research on design method and electromagnetic vibration of six-phase fractional-slot concentrated-winding PM motor suitable for ship propulsion," *IEEE Access*, vol. 4, pp. 8535–8543, 2016, doi: [10.1109/ACCESS.2016.2636341](https://doi.org/10.1109/ACCESS.2016.2636341).
- [15] D. Kong, Z. Shuai, W. Li, and D. Wang, "Electromagnetic vibration characteristics analysis of a squirrel-cage induction motor under different loading conditions," *IEEE Access*, vol. 7, pp. 173240–173248, 2019, doi: [10.1109/ACCESS.2019.2956950](https://doi.org/10.1109/ACCESS.2019.2956950).
- [16] Z. M. Wen, "Research and implementation of free interface mode synthesis," M.S. thesis, School Mech. Sci. Eng., Huazhong Univ. Sci. Technol., Wuhan, Hubei, China, 2014.
- [17] C. Zhou, "Modeling and analysis of vehicle drive axle system modal comprehensive dynamics," *J. Vib. Shocks*, vol. 36, no. 9, pp. 7–12, 2017.
- [18] K. K. Singh, S. S. Kulkarni, V. Kartik, and R. Singh, "A free interface component mode synthesis approach for determining the micro-end mill dynamics," *J. Micro Nano-Manuf.*, vol. 6, no. 3, Sep. 2018, Art. no. 031005, doi: [10.1115/1.4040468](https://doi.org/10.1115/1.4040468).
- [19] Y. Yu, "The dynamic simulation research for fairing separation process based on component mode synthesis," M.S. thesis, School Aeronaut. Astronaut., Dalian Univ. Technol., Dalian, Liaoning, China, 2015.
- [20] X. H. Sun, "Frequency domain modal parameter identification and software implementation," Ph.D. dissertation, Graduate School College Aersp. Eng., Nanjing Univ. Aeronaut. Astronaut., Nanjing, Jiangsu, China, 2010.



JIAN ZHAO received the B.Eng. degree from Hunan University, Changsha, China, in 1987, the M.Sc. degree from the Taiyuan University of Science and Technology, Taiyuan, China, in 1992, and the Ph.D. degree from Tianjin University, Tianjin, China, in 2007, all in mechanical engineering.

She became an Associate Professor with the School of Mechanical Engineering, Taiyuan University of Science and Technology, in 2001, and a Professor with the School of Energy and Mechanical Engineering, Tianjin Chengjian University, in 2008. She is currently a Professor with the School of Control and Mechanical Engineering, Tianjin Chengjian University. Her research interests include structure dynamics, measurement and control technology of vibration and noise, and dynamic monitoring and intelligent diagnosis.



ZHIBIN WANG received the B.Eng. degree from the Taiyuan University of Science and Technology, Taiyuan, China, in 2018. He is currently pursuing the master's degree with the School of Control and Mechanical Engineering, Tianjin Chengjian University. His current research interests include the condition monitoring, diagnosis, and control technology of engineering construction equipment.



HAIQIANG LIU received the B.Eng. degree from Weifang University, Weifang, China, in 2016, and the M.S. degree from Tianjin Chengjian University, Tianjin, China, in 2019. He is currently working as an Assistant Researcher at the Mechanical Engineering Laboratory, School of Control and Mechanical Engineering, Tianjin Chengjian University. His main research interests include dynamic testing and intelligent diagnosis.



JINGJUAN DU received the Ph.D. degree from Tianjin University. Her main research interests include the electromagnetic field design and analysis of high-speed motors for electric vehicles, the design of fluid cooling methods, and the application of coupled thermal analysis.



FAN NING received the B.Eng. degree from the Taiyuan University of Technology, Taiyuan, China, in 2018. He is currently pursuing the master's degree with the School of Control and Mechanical Engineering, Tianjin Chengjian University. His current research interests include construction status monitoring, diagnosis, and control technology.



XUEWU HONG received the M.S. degree from Tianjin Chengjian University, Tianjin, China, in 2017. Since 2017, he has been an Assistant Researcher with the School of Control and Mechanical Engineering, Institute of Modern Manufacturing and Measurement and Control Technology, Tianjin Chengjian University. His main research interests include vibration and noise measurement and control technology.



MING YU received the B.Eng. degree from Xidian University, Xi'an, China, in 1986, and the M.S. degree, in 1992.

From 1998 to 2007, he was a Senior Engineer with the 33rd Research Institute, China Electronics Technology Group Corporation. Since 2007, he has been an Associate Professor with the School of Computer and Information Engineering, Tianjin Chengjian University. His main research interests include information processing and fault diagnosis.

...